JACS
JOURNAL OF THE AMERICAN CHEMICAL SOCIETY

Subscriber access provided by American Chemical Society

Article

Mechanism of 1,3-Migration in Allylperoxyl Radicals: Computational Evidence for the Formation of a Loosely Bound Radical–Dioxygen Complex

Santiago Olivella, and Albert Sol

J. Am. Chem. Soc., **2003**, 125 (35), 10641-10650• DOI: 10.1021/ja030171e • Publication Date (Web): 06 August 2003

Downloaded from http://pubs.acs.org on March 29, 2009

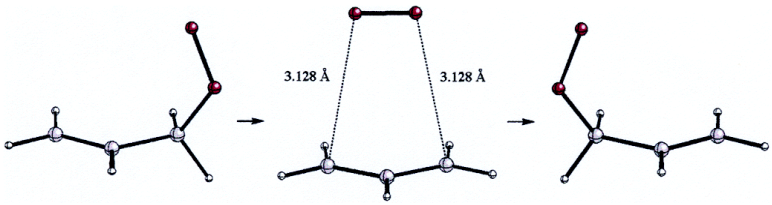

More About This Article

Additional resources and features associated with this article are available within the HTML version:

- Supporting Information
- Links to the 1 articles that cite this article, as of the time of this article download
- Access to high resolution figures
- Links to articles and content related to this article
- Copyright permission to reproduce figures and/or text from this article

View the Full Text HTML

ACS Publications
High quality. High impact.

Journal of the American Chemical Society is published by the American Chemical Society. 1155 Sixteenth Street N.W., Washington, DC 20036

J|A|C|S
ARTICLES
Published on Web 08/06/2003

Mechanism of 1,3-Migration in Allylperoxyl Radicals: Computational Evidence for the Formation of a Loosely Bound Radical−Dioxygen Complex

Santiago Olivella*,† and Albert Solé*,‡

Contribution from the Institut d'Investigacions Químiques i Ambientals de Barcelona, CSIC, Jordi Girona 18, 08034-Barcelona, Catalonia, Spain and Centre Especial de Recerca en Química Teòrica i Departament de Química Física, Universitat de Barcelona, Martí i Franquès 1, 08028-Barcelona, Catalonia, Spain

Received March 17, 2003; E-mail: sonqtc@cid.csic.es; asole@qf.ub.es

Abstract: The three pathways postulated for 1,3-migration of the peroxyl group in the allylperoxyl radical (**1a**), a key reaction involved in the spontaneous autoxidation of unsaturated lipids of biological importance, have been investigated by means of quantum mechanical electronic structure calculations. According to the barrier heights calculated from RCCSD(T)/6-311+G(3df,2p) energies with optimized molecular geometries and harmonic vibrational frequencies determined at the UMP2/6-311+G(3df,2p) level, the allylperoxyl rearrangement proceeds by fragmentation of **1a** through a transition structure (**TS1**) with a calculated $\Delta H^{\ddagger}$(298 K) of 21.7 kcal/mol to give an allyl radical−triplet dioxygen loosely bound complex (**CX**). In a subsequent step, the triplet dioxygen moiety of **CX** recombines at either end of the allyl radical moiety to convert the complex to the rearranged peroxyl radical (**1a′**) or to revert to the starting peroxyl radical **1a**. **CX** shows an electron charge transfer of 0.026 e in the direction allyl → O_2. The dominant attractive interactions holding in association the allyl radical−riplet dioxygen pair in **CX** are due chiefly to dispersion forces. The ΔH(298 K) for dissociation of **CX** in its isolated partners, allyl radical and triplet dioxygen, is predicted to be at least 1 kcal/mol. The formation of **CX** prevents the diffusion of its partners and maintains the stereocontrol along the fragmentation-recombination processes. The concerted 1,3-migration in allylperoxyl radical is predicted to take place through a five-membered ring peroxide transition structure (**TS2**) showing two long C−O bonds. The $\Delta H^{\ddagger}$(298 K) calculated for this pathway is less favorable than the fragmentation−recombination pathway by 1.9 kcal/mol. The cyclization of **1a** to give a dioxolanyl radical intermediate (**2a**) is found to proceed through a five-membered ring transition structure (**TS3**) with a calculated $\Delta H^{\ddagger}$(298 K) of 33.9 kcal/mol. Thus, the sequence of ring closure **1a** → **2a** and ring opening **2a** → **1a′** is unlikely to play any significant role in allylperoxyl rearrangement **1a** → **1a′**. In the three pathways investigated, the energy of the transition structure is predicted to be somewhat lower in either heptane or aqueous solution than in the gas phase. Although the energy lowering calculated for **TS1** is smaller than the calculated for **TS2** and **TS3**, it is very unlikely that the solvent effects may reverse the predicted preference of the fragmentation−recombination pathway over the concerted and stepwise ring closure-ring opening mechanisms.

Introduction

Allylperoxyl radicals (**1**) are intermediates which are formed when unsaturated organic compounds react with molecular oxygen (autoxidation). They are thus involved in processes as diverse as the development of rancidity in unsaturated fats, the drying of paints, and the perishing of rubber. In recent years, the chemistry of allylperoxyl radicals involved in the spontaneous autoxidation of unsaturated lipids of biological importance has received renewed interest because they have been implicated in peroxidative destruction of cell membranes, DNA and protein modification, radiation damage, aging and age pigment formation, tumor initiation, and the deposition of arterial plaque associated with low-density lipoprotein modification.[1,2]

Allylperoxyl radicals are known to undergo [2,3]-rearrangements (e.g., **1** → **1′**) in nonpolar aprotic solvents (e.g., hexane)

1 **1'**

in which the peroxyl unit migrates across the allylic backbone (Schenk rearrangement).[3] The main practical importance of this process lies in its effect on the composition ratio of hydroper-

† Institut d'Investigacions Químiques i Ambientals de Barcelona, CSIC.
‡ Centre Especial de Recerca en Química Teòrica i Departament de Química Física, Universitat de Barcelona.

(1) Porter, N. A.; Mills, K. A.; Carter, R. L. *J. Am. Chem. Soc.* **1994**, *116*, 6690−6696.
(2) Porter, N. A.; Caldwell, S. E.; Mills, K. A. *Lipids* **1995**, *30*, 277−290.

Scheme 1

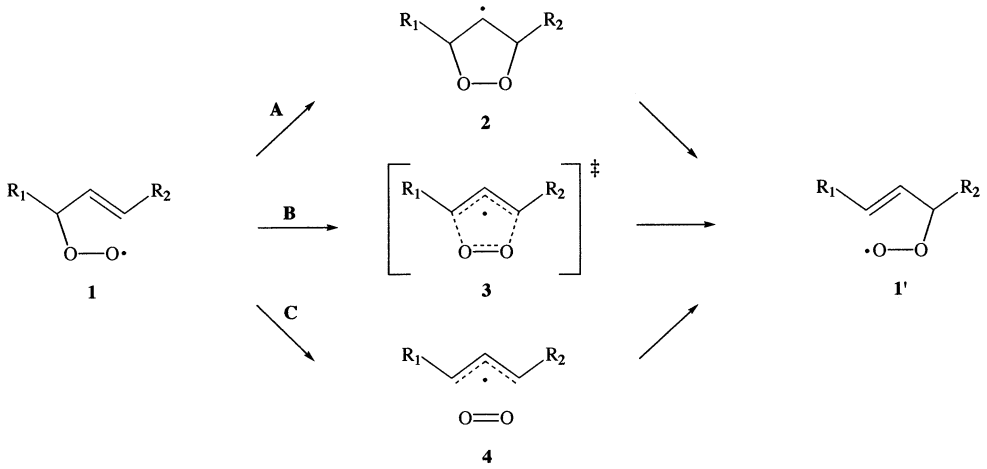

oxides formed in the autoxidation of unsaturated lipids. Despite the fact that [2,3]-rearrangements have been known since the late 1950s, the mechanism is still under debate.[4] As shown in Scheme 1, three mechanisms have been most often suggested for allylperoxyl rearrangement.[5−11] The first (pathway **A**) consists of a stepwise process involving a carbon centered dioxolanyl radical intermediate (**2**), which subsequently undergoes β-scission. Another viable mechanism (pathway **B**) consists of a concerted mechanism involving a five-membered ring peroxide transition state (**3**). Finally, an alternative stepwise process (pathway **C**) has also been suggested in which the peroxyl radical undergoes β-scission to give an allyl radical and triplet dioxygen pair species (**4**). In a subsequent step, the triplet dioxygen recombines at either end of the allyl radical to convert it to the rearranged peroxyl radical (**1′**) or to revert to the starting peroxyl radical **1**.

Brill[5] and Porter[6] provided evidence that the migration does not occur in a stepwise process by cyclization of the allylperoxyl radical to produce a dioxolanyl radical intermediate **2** (pathway **A** in Scheme 1) since authentic dioxolanyl radicals undergo reactions to give products not observed in the rearrangement product mixture. Beckwith, Davies, and co-workers[7] subsequently reported an ESR investigation on the cholesterol allylperoxyl rearrangement under $(^{18}O)_2$ atmosphere and suggested that the reaction involves a concerted sigmatropic [2,3]-allylperoxyl rearrangement. Porter and Wujek[8] proposed that the allylperoxyl rearrangement proceeds through a concerted transition state like **3** (pathway **B** in Scheme 1). Evidence to support this view is the fact that, in optically pure acyclic allylic peroxyl radicals, the rearrangement is a highly stereoselective process.[9]

To the best of our knowledge, only one theoretical paper has been devoted to the study of the mechanism of the allylperoxyl rearrangement. Specifically, the prototype 1,3-migration of the peroxyl unit in the allylperoxyl radical (**1**, R_1═R_2═H), designated by **1a**, has been studied theoretically by Boyd et al.[10] Employing single-point second- and third-order Moeller−Plesset perturbation theory with standard 6-31G(d,p) basis set, performed at the geometries optimized by using the unrestricted Hartree−Fock (UHF) method with standard 6-31G(d) basis set, those authors failed to find a concerted transition state like **3** proposed for the rearrangement. The calculations revealed the 1,2-dioxolanyl-4-yl radical (**2**, R_1═R_2═H), designated by **2a**, to be close in energy to that of radical **1a** but the lowest energy pathway from **1a** to **2a** proceeds over a barrier of almost 41 kcal/mol. Since earlier calculations[11] indicated that the C−O bond energy in **1a** is about 21.5 kcal/mol, significantly lower than the barrier calculated for the rearrangement through **2a**, Boyd and co-workers suggested that the allylperoxyl rearrangement proceeds by fragmentation of **1a** to give the allyl radical and triplet dioxygen, which subsequently recombine leading to the rearranged peroxyl radical **1a′** (pathway **C** in Scheme 1). The authors concluded that the observed high degree of stereoselectivity of the rearrangement must result from a cage effect, wherein the diffusion of the allyl radical−triplet dioxygen pair is prevented due to the caging by the solvent. In this mechanism, recombination of the allyl radical and dioxygen of an initial radical−dioxygen pair occurs with stereochemical memory to return to the starting peroxyl or to give the rearranged peroxyl radical. However, the authors pointed out that there is no precedent in the literature to support this notion. On the other hand, since the attempts to locate the concerted transition structure were performed at the UHF level of theory and it is likely that an adequate description of the electronic structure of such a transition structure requires inclusion of the electron correlation, the existence of a concerted pathway for the 1,3-migration in the allylperoxyl radical cannot be fully discarded.

In latter work, Porter et al.[12] assumed that the allylperoxyl rearrangement proceeds by a fragmentation−recombination mechanism (pathway **C** in Scheme 1) and reported stereochemical-oxygen labeling studies indicating that solvent viscosity affects the partitioning between escape by difussion and recombination of the allyl radical−dioxygen caged pair. An increase in solvent viscosity results in a decrease in escape

(3) (a) Schenk, G. O.; Neumuller, O.-A.; Eisfeld, W. *Angew. Chem.* **1958**, *70*, 595. (b) Schenk, G. O.; Neumuller, O.-A.; Eisfeld, W. *Justus Liebigs Ann. Chem.* **1958**, *618*, 202.
(4) Walton, J. C. *Acc. Chem. Res.* **1998**, *31*, 99−107.
(5) Brill, W. E. *J. Chem. Soc., Perkin Trans. 2* **1984**, 621−627.
(6) Porter, N. A.; Zuraw, P. J. *J. Chem. Soc., Chem Commun.* **1985**, 1472.
(7) Beckwith, A. L. J.; Davies, A. G.; Davison, I. E. G.; Maccoll, A.; Mruzek, M. H. *J. Chem. Soc., Perkin Trans. 2* **1989**, 815−824.
(8) Porter, N. A.; Wujek, J. S. *J. Org. Chem.* **1987**, *52*, 5085.
(9) Porter, N. A.; Kaplan, J. K.; Dussault, P. H. *J. Am. Chem. Soc.* **1990**, *112*, 1266−1267.
(10) Boyd, S. L.; Boyd, R. J.; Barclay, L. R. C.; Porter, N. A. *J. Am. Chem. Soc.* **1993**, *115*, 687−1267.
(11) Boyd, S. L.; Boyd, R. J.; Barclay, L. R. C. *J. Am. Chem. Soc.* **1990**, *112*, 5724.
(12) (a) Mills, K. A.; Caldwell, S. E.; Dubay, G. R.; Porter, N. A *J. Am. Chem. Soc.* **1992**, *114*, 9689−9691. (b) Porter, N. A.; Mills, K. A.; Caldwell, S. E.; Dubay, G. R. *J. Am. Chem. Soc.* **1994**, *116*, 6690−6696.

product and an identical increase in pair readdition product formed with stereocontrol. This viscosity dependence observed gives evidence in support of a cage effect in the allylperoxyl rearrangement. More recently, Lowe and Porter[13] have investigated the course of the peroxyl oxygens during the allylperoxyl rearrangement of an allylic hydroperoxide having a specific hydroperoxide oxygen labeled. The results of that investigation showed that the rearrangement is temperature dependent, reactions carried out at lower temperatures proceeding with less loss of label to the atmosphere and with more positional selectivity of the label transfer. Lowe and Porter Assumed for the rearrangement a mechanism involving competition between a pathway connecting the reactant and product allylperoxyl radicals directly by a process in which the terminal oxygen of the reactant is transferred to the product proximal position and a pathway involving fragmentation of allylperoxyl to a pair species which can collapse to allylperoxyl with scrambling of label or escape to give the allyl radical and dioxygen. The temperature dependence on positional selectivity of the label transfer and loss of label provided an estimate of the rate constants' ratio for the two pathways. Estimation of this rate constants' ratio at 20, 40, and 60 °C followed by Eyring analysis provided approximate $\Delta\Delta H^{\ddagger}$ and $\Delta\Delta S^{\ddagger}$ values (i.e., $\Delta H^{\ddagger}_2 - \Delta H^{\ddagger}_1 = 9.0$ kcal/mol and $\Delta S^{\ddagger}_2 - \Delta S^{\ddagger}_1 = 26$ eu) for the two competitive pathways.

At this point, several questions naturally arise: What is the energy barrier involved in the fragmentation of allylperoxyl radical to give allyl radical and triplet dioxygen? Do the allyl radical and the triplet dioxygen form a caged pair species, and if this turns out to be the case, is the caged pair a stationary point on the ground-state potential energy surface (PES), and what is the nature of the attractive interactions holding in association the allyl radical and the triplet dioxygen in the caged pair? Does there exist a transition structure for the concerted allylperoxyl rearrangement at the electron correlated level of theory? To answer these questions, we investigated the stationary points on the $C_3H_5O_2^{\bullet}$ ground-state PES most relevant to the 1,3-migration of the peroxyl unit in **1a** by means of high-level ab initio quantum mechanical electronic structure calculations. We report here the energetic and structural results of this theoretical investigation. The findings presented demonstrate that a loosely bound radical−triplet dioxygen complex mediates the allylperoxyl radical rearrangement.

Computational Details

A high-level treatment of electron correlation energy is mandatory to reliably describe the expected weak interactions between the allyl radical and triplet dioxygen in the radical−dioxygen caged pair postulated by Boyd and Porter as intermediate in the allylperoxyl rearrangement. Though density functional theory (DFT) is more and more commonly used as a very efficient computational method for the study of molecules and bulk materials, its applications to weakly bonded systems remain rather sparse in the literature, except studies that consider hydrogen bonding.[14] On the contrary, second-order Moeller−Plesset perturbation theory[14] (MP2) in conjunction with a large basis set is nowadays usually accepted as a good starting point to account for the correlation effects required to describe weakly bonded systems.[15−17] Therefore, we decided to employ the spin-unrestricted version of the MP2 method, designated UMP2, with the split-valence 6-311+G(3df,2p) basis set,[18] which includes a single diffuse sp shell on carbon and oxygen atoms,[19] triple d-polarization and a single additional f-polarization on carbon and oxygen atoms, and double p-polarization on hydrogen atoms.

The geometries of the relevant stationary points on the ground-state $C_3H_5O_2^{\bullet}$ PES were initially optimized at the UMP2/6-311+G(3df,2p) level employing analytical gradient procedures.[21,22] All the stationary points were characterized by their harmonic vibrational frequencies as minima or saddle points. All of these calculations were performed with the GAUSSIAN 98 program package.[23]

While the UMP2 method, based on a reference unrestricted Hartree−Fock (UHF) single determinant, gives an adequate description of the PES in those regions where the nondynamical electron correlation effects are expected to be small, it is unlikely that the UMP2 method can provide an adequate description of the allylperoxyl dissociation to a doublet allyl radical and triplet dioxygen.[10] Therefore, the transition structure for this pathway was reoptimized by use of a multiconfiguration self-consistent field wave function of the complete active space (CASSCF) class[24] with the 6-311+G(3df,2p) basis set. The CAS was selected following the procedure suggested by Anglada and Bofill,[25] based on the fractional occupation of the natural orbitals generated from the first-order density matrix calculated from an initial multireference single- and double-excitation configuration interaction wave function correlating all valence electrons. The active space consisted of 11 electrons and 9 orbitals: the three electrons and three orbitals involved in the π system of the allyl radical unit plus eight electrons and six orbitals of the dioxygen unit. Distribution of the corresponding 11 *active* electrons among these 9 *active* orbitals leads to a wave function designated by CASSCF(11,9). To obtain comparable energies, single-point CASSCF(11,9) calculations were carried out for some stationary points at the UMP2/6-311+G(3df,2p) optimized geometries. All CASSCF calculations were performed by using GAMESS system of programs.[26]

To incorporate the effect of dynamical valence-electron correlation on the relative energy ordering of the stationary points, second-order multiconfigurational perturbation theory calculations (CASPT2)[27] based on the CASSCF(11,9) reference function were carried out. CASPT2 single-point energies were calculated at the geometries optimized at either the CASSCF(11,9)/6-311+G(3df,2p) or UMP2/6-311+G(3df,2p) level, using the 6-311+G(3df,2p) basis set. To take into account the different multiplicities of the dissociation products (i.e., doublet allyl radical and triplet dioxygen), the CASPT2-g1 procedure with the full Hartree−Fock matrix was used in the construction of the zeroth-order

(13) Lowe, J. R.; Porter, N. A. *J. Am. Chem. Soc.* **1997**, *119*, 11534−11535.
(14) Wesolowsky, T. A.; Parisel, O.; Ellinger, Y.; Weber, J. *J. Phys. Chem. A* **1997**, *101*, 7818−7825.
(15) (a) Moller, C.; Plesset, M. *Phys. Rev.* **1934**, *46*, 618. (b) Pople, J. A.; Binkley, J. S.; Seeger, R. *Int. J. Quantum Chem., Symp.* **1976**, *10*, 1.
(16) Hobza, P.; Zahradnik, R. *Chem. Rev.* **1988**, *88*, 871.
(17) Hobza, P.; Selze, H. L.; Schlag, E. W. *Chem. Rev.* **1994**, *94*, 1767.
(18) Chalasinski, G.; Szczesniak, M. *Chem. Rev.* **1994**, *94*, 1723.
(19) Frisch, M. J.; Pople, J. A.; Binkley, J. S. *J. Chem. Phys.* **1984**, *80*, 3265.
(20) Hehre, W. J.; Radom, L.; Schleyer, P. v. R.; Pople, J. A. *Ab Initio Molecular Orbital Theory*; John Wiley: New York, 1986; pp 86−87.
(21) Schlegel, H. B. *J. Comput. Chem.* **1982**, *3*, 214.
(22) Bofill, J. M. *J. Comput. Chem.* **1994**, *15*, 1.
(23) Frisch, M. J.; Trucks, G. W.; Schlegel, H. B.; Scuseria, M. A.; Robb, M. A.; Cheeseman, J. R.; Zakrzewski, V. G.; Montgomery, J. A.; Stratmann, R. E.; Burant, J. C.; Dapprich, S.; Milliam, J. M.; Daniels, A. D.; Kudin, K. N.; Strain, M. C.; Farkas, O.; Tomasi, J.; Barone, V.; Cossi, M.; Cammi, R.; Mennucci, B.; Pomelli, C.; Adamo, C.; Clifford, S.; Ochterski, J.; Petersson, G. A.; Ayala, P. Y.; Cui, Q.; Morokuma, K.; Malick, D. K.; Rabuck, A. D.; Raghavachari, K.; Foresman, J. B.; Cioslowski, J.; Ortiz, J. V.; Stefanow, B. B.; Liu, G.; Liashenko, A.; Piskorz, P.; Komaromi, A.; Gomperts, R.; Martin, R. L.; Fox, D. J.; Keith, T.; Al-Laham, M. A.; Peng, C. Y.; Nanayakkara, A.; Gonzalez, C.; Challacombe, M.; Gill, P. M. W.; Johnson, B. G.; Chen. W.; Wong, M. W.; Andres, J. L.; Head-Gordon, M.; Replogle, E. S.; Pople, J. A. *GAUSSIAN 98*, revision A.11; Gaussian, Inc.: Pittsburgh, PA, 1998.
(24) For a review, see: Roos, B. O. *Adv. Chem. Phys.* **1987**, *69*, 399.
(25) Anglada, J. M.; Bofill, J. M. *Theor. Chim. Acta* **1995**, *92*, 369.
(26) Schmidt, M. W.; Baldrige, K. K.; Boatz, J. A.; Elbert, S. T.; Gordon, M. S.; Jensen; J.; Koseki, S.; Matsunaga, N.; Nguyen, K. A.; Su, S.; Windus, T. L.; Dupuis, M.; Montgomery, J. A. *J. Comput. Chem.* **1993**, *14*, 1347.
(27) (a) Anderson, K.; Malmqvist, P.-A.; Roos, B. O.; Sadlej, A. J.; Wolinski, K. *J. Phys. Chem.* **1990**, *94*, 5483. (b) Anderson, K.; Malmqvist, P.-A.; Roos, B. O. *J. Chem. Phys.* **1992**, *96*, 1218.

Hamiltonian.[28] The CASPT2 computations were performed with the MOLCAS 5 program package.[29]

Further, we investigated the effect of computing the electron correlation at higher levels of theory on the relative energy ordering of the stationary points located at the UMP2/6-311+G(3df,2p) level. To this end, single-point (frozen core) coupled-cluster[30] calculations including all single and double excitations, based on a reference UHF single determinant, together with a perturbative treatment of all connected triple excitations,[31] designated UCCSD(T), were carried out with the 6-311+G(3df,dp) basis set. Finally, total energies for relevant stationary points were also evaluated from partially spin-adapted CCSD-(T) calculations based on a restricted open-shell Hartree−Fock (ROHF) reference determinant,[32] designated RCCSD(T), to accomplish the spin contamination problem in UCCSD(T) wave functions.[33] The UCCSD-(T) calculations were carried out with GAUSSIAN 98, whereas the MOLPRO 98[34] program package was employed for the RCCSD(T) calculations.

Zero-point vibrational energies (ZPVEs) were determined from the harmonic vibrational frequencies calculated at the UMP2/6-311+G-(3df,2p) level. Our best total energies at 0 K correspond to the sum of the RCCSD(T)/6-311+G(3df,2p) energy and ZPVE correction. Thermal corrections to enthalpy, absolute entropies, and Gibbs free-energy values were obtained assuming ideal gas behavior from the unscaled harmonic frequencies and moments of inertia by standard methods.[35] A standard pressure of 1 atm was taken in the absolute entropies calculations.

To examine the characteristics of the bonding and interactions in the most relevant structures, we have also performed an analysis of the electron charge density within the framework of the topological theory of atom in molecules (AIM)[34] making use of a locally modified version[37] of the PROAIM and EXTREME programs of Bader et al.[38] and the MORPHY 97 program.[39] The **Z** density matrix obtained from UMP2 gradient calculations with the 6-311+G(3df,2p) basis set, an effective correlated density matrix,[40] were used in this analysis.

Preliminary Test for the Complex of Benzene with Oxygen. To confirm the reliability of the UMP2/6-311+G(3df,2p) theoretical procedure, we tested it on the complex of benzene with dioxygen. Triplet O_2 ($^3\Sigma_g^-$) and benzene are known to form a weak 1:1 complex in the ground state, which is detected through the appearance of a charge transfer band with a band at 219 nm.[41] A dissociation energy D_0 of 1.6 ± 0.3 kcal/mol has been measured by Grover and co-workers for the benzene−O_2 complex in the gas phase.[42]

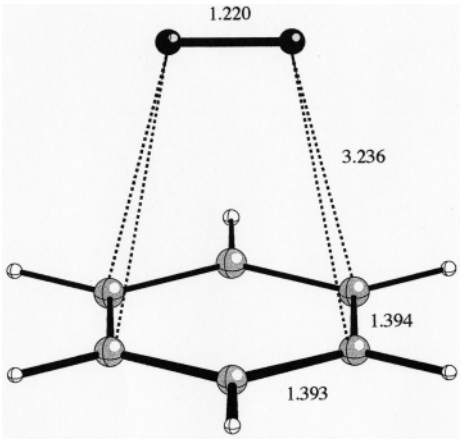

Figure 1. Selected parameters of the UMP2/6-311+G(3df,2p) optimized geometry of the complex of benzene with triplet dioxygen. Distances are given in angstroms.

Figure 1 shows the lowest-energy equilibrium geometry calculated for the ground-state benzene−O_2 complex. This structure posseses C_{2v} symmetry and is a triplet state of B_2 symmetry. It has a parallel arrangement with the O_2 on a symmetry plane bisecting two C−C bonds. A configuration with the O_2 on a symmetry plane containing two opposite C−H bonds turned out to be only 0.01 kcal/mol higher in energy. The distance between the centers-of-mass of benzene and O_2 (R_{BO}) is 3.103 Å, and the shortest C−O distances are found to be 3.236 Å. As expected from these long distances between the benzene and O_2 moieties, the structural perturbation of the two partners in the benzene−O_2 complex are insignificant as compared with the separated species. In fact, the C−C and O−O bonds undergo a lengthening of only 0.001 and 0.002 Å, respectively. No experimental data are available concerning the geometry of the benzene−O_2 complex. Previous theoretical calculations at the UMP2 level of theory with different basis sets by Granucci and Persico[43] and Wesolowsky et al.[14] predicted for the R_{BO} distance the values of 3.36 and 3.21 Å, respectively. In these calculations, the experimental geometries of benzene and O_2 were assumed and kept fixed along the geometry optimization of the benzene−O_2 complex.

At the UMP2/6-311+G(3df,2p) level, the energy of the benzene−O_2 complex lies 2.9 kcal/mol below the sum of the energies of the isolated partners, benzene and O_2 (Table S1, Supporting Information). It is worth noting that the amount of spin contamination in the reference UHF wave function was found to be very small; thus the expectation value of the spin-squared operator S^2 was calculated to be 2.050, which is very close to the value of 2.0 for a pure triplet state. By means of the counterpoise method,[44] a basis set superposition error (BSSE) correction of 1.2 kcal/mol was calculated at the UMP2/6-311+G(3df,2p) level. This BBSE correction reduces the predicted stabilization energy to 1.7 kcal/mol. Inclusion in the latter value of a ZPVE correction of 0.4 kcal/mol (Table S1, Supporting Information) leads to a 0 K stabilization energy of 1.3 kcal/mol, which is in reasonable agreement with the experimental dissociation energy of 1.6 ± 0.3 kcal/mol.

The net atomic charges evaluated by using the AIM population analysis of the effective UMP2/6-311+G(3df,2p) electron density showed an electron charge transfer in the benzene−O_2 complex of only 0.026 e in the direction benzene → O_2. This is consistent with previous theoretical findings indicating that the dominant attractive interactions holding in association the benzene and O_2 partners in the loosely bound benzene−O_2 complex arise mainly from dispersion forces.[14,43]

(28) Anderson, K. *Theor. Chim. Acta* **1995**, *91*, 31.
(29) Andersson, K.; Barysz, M.; Bernhardsson, A.; Blomberg, M. R. A.; Cooper, D. L.; Fleig, T.; Fülscher, M. P.; DeGraaf, C.; Hess, B. A.; Karlström, G.; Lindh, R.; Malmqvist, P.-Å.; Neogrády, P.; Olsen, J.; Roos, B. O.; Sadlej, A. J.; Schütz, M.; Schimmelpfennig, B.; Seijo, L.; Serrano-Andrés, L.; Siegbahn, P. E. M.; Stålring, J.; Thorsteinsson, T.; Veryazov, V.; Widmark, P.-O. *MOLCAS*, version 5; Lund University: Sweden, 2000.
(30) For a review, see: Bartlett, R. J. *J. Phys. Chem.* **1989**, *93*, 1967.
(31) Raghavachari, K.; Trucks, G. W.; Pople. J. A.; Head-Gordon, M. *Chem. Phys. Lett.* **1989**, *157*, 479.
(32) Knowles, P. J.; Hampel, C.; Werner, H.-J. *J. Chem. Phys.* **1993**, *99*, 5219.
(33) (a) Purvis, G. D.; Bartlett, R. J.; *J. Chem. Phys.* **1982**, *76*, 1910. (b) Hampel, C.; Peterson, K. A.; Werner, H.-J. *Chem. Phys. Lett.* **1992**, *190*, 1. (c) Deegan, M. J. O.; Knowles, P. J. *Chem. Phys. Lett.* **1994**, *227*, 321.
(34) Werner, H.-J.; Knowles, P. J.; Almlöf, J.; Amos, R. D.; Berning, A.; Cooper, D. L.; Deegan, M. J. O.; Dobbyn. A. J.; Eckert, S. T.; Hampel, C.; Leininger, C.; Lindh, R.; Lloyd, A. W.; Meyer, W.; Mura, M. E.; Nicklass, A.; Palmeiri, P.; Peterson, K. A.; Pitzer, R.; Pulay, P.; Rauhaut, G.; Schütz, M.; Stoll, H.; Stone, A. J.; Thorsteinsson, T. *MOLPRO*, version 98.1; University of Stuttgart: Germany, 1998.
(35) For example, see: McQuarrie, D. *Statistical Mechanics*; Harper and Row: New York, **1986**.
(36) Bader, R. F. W. *Atoms in Molecules: A Quantum Theory;* Clarendon: Oxford, U.K., **1990**.
(37) Mota, F. Universitat de Barcelona, unpublished work.
(38) (a) Biegler-König, F. W.; Bader, R. F. W.; Tang, T.-H. *J. Comput. Chem.* **1982**, *3*, 317. (b) Bader, R. F. W.; Tang, T.-H.; Tal, Y.; Biegler-König, F. W. *J. Am. Chem. Soc.* **1982**, *104*, 946.
(39) (a) MORPHY 97: Popelier, P. L. A. with contributions from Bone, R. G. A.; UMIST: Manchester, U.K., 1997. (b) Popelier, P. L. A. *Comput. Phys. Commun.* **1998**, *108*, 180.
(40) For example, see: Wiberg, K.B.; Hadad, C. M.; LePage, T.; Breneman, C. M.; Frisch, M. J. *J. Phys. Chem.* **1992**, *96*, 671.
(41) Birks, J. B.; Pantos, E.; Hamilton, T. D. S. *Chem. Phys. Lett.* **1973**, *20*, 544.
(42) Grover, J. R.; Hagenow, G.; Walters, E. A. *J. Chem. Phys.* **1992**, *97*, 628−642.
(43) Granucci, G.; Persico, M. *Chem. Phys. Lett.* **1993**, *205*, 331−336.
(44) Boys, S. F.; Bernardi, F. *Mol. Phys.* **1970**, *19*, 553.

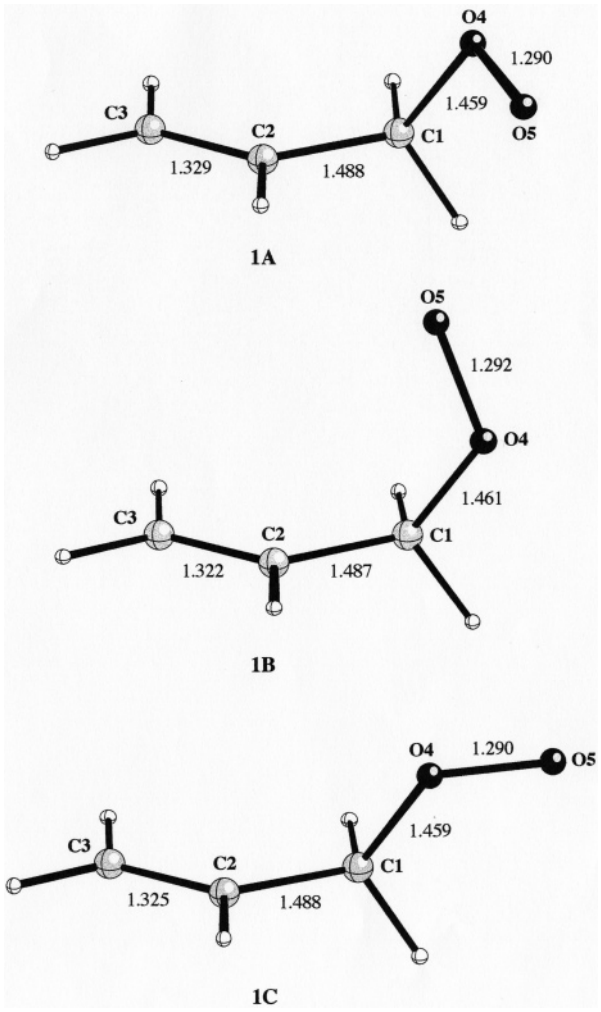

Figure 2. Selected parameters of the UMP2/6-311+G(3df,2p) optimized geometries of the most relevant conformational minima of the allylperoxyl radical. Distances are given in angstroms.

We conclude that the UMP2 level of theory with the 6-311+G-(3df,2p) basis set might provide an adequate description of the weak interactions between the allyl radical and triplet dioxygen caged pair postulated by Boyd and Porter.[10]

Results and Discussion

Selected geometrical parameters of the most relevant stationary points located on the $C_3H_5O_2^{\bullet}$ ground-state PES for the 1,3-migration of the peroxyl unit in **1a** are shown in Figures 2−6 (bond lengths in Å), which are computer-generated plots of the optimized geometries at either the UMP2 or CASSCF(11,9) levels of theory with the 6-311+G(3df,2p) basis set. The Cartesian coordinates of all structures reported in this paper are available as Supporting Information, and the total energies calculated at various levels of theory with the 6-311+G(3df,dp) basis set, as well as the ZPVEs and the electric dipole moments of these structures, are collected in Table S2 (Supporting Information). Relative energies calculated at different levels of theory for the most relevant stationary points are summarized in Tables 1 and 2, whereas those for less relevant stationary points are collected in Table S3 (Supporting Information). For some of the most relevant stationary points, Table 3 gives the relative energies calculated at the RCCSD(T)/6-311+G(3df,dp) level (ΔU), the relative ZPVEs ($\Delta ZPVE$), the relative energies

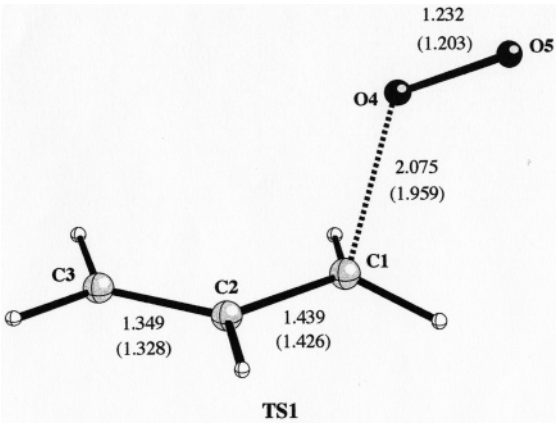

Figure 3. Selected parameters of the CASSCF(11,9)/6-311+G(3df,2p) optimized geometry of the transition structure for the fragmentation of the allylperoxyl radical to give an allyl radical and a triplet dioxygen. The UMP2/6-311+G(3df,2p) optimized parameters are given in parentheses. Distances are given in angstroms.

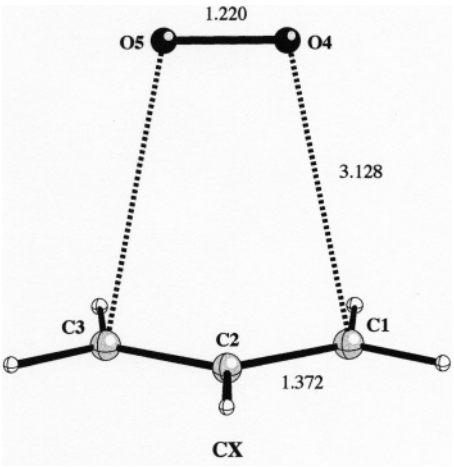

Figure 4. Selected parameters of the UMP2/6-311+G(3df,2p) optimized geometriey of the loosely bound allyl radical−triplet dioxygen complex. Distances are given in angstroms.

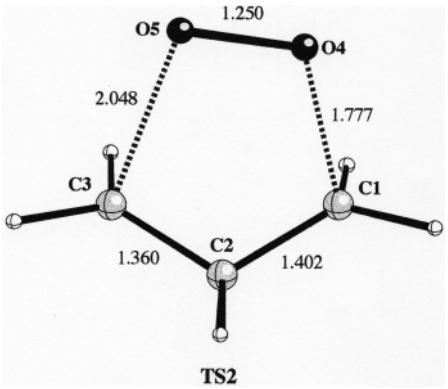

Figure 5. Selected parameters of the UMP2/6-311+G(3df,2p) optimized geometry of the transition structure for the concerted 1,3-migration in the allylperoxyl radical. Distances are given in angstroms.

at 0 K (ΔE), and the relative enthalpies (ΔH) and Gibbs free energies (ΔG) calculated at 298 K. Figure 7 summarizes the ΔE profiles of the three different pathways leading to the 1,3-migration in **1a**. Calculated topological properties of the bond critical points for the most relevant structures, determined from AIM analysis of the effective UMP2/6-311+G(3df,dp) electron charge density, are given in Table S4 (Supporting Information).

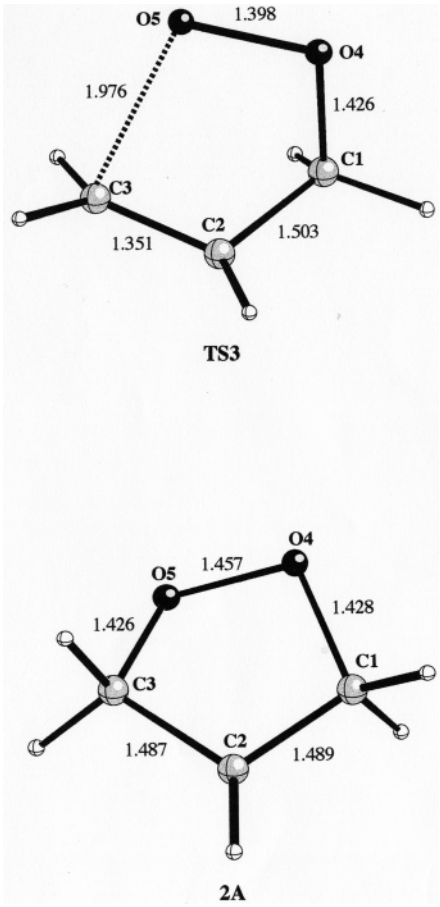

Figure 6. Selected parameters of the UMP2/6-311+G(3df,2p) optimized geometries of the 1,2-dioxolanyl-4-yl radical intermediate (**2A**) and the transition structure (**TS3**) connecting this intermediate and the allylperoxyl radical. Distances are given in angstroms.

Table 1. Relative Energies (kcal/mol) Calculated at Different Levels of Theory with the 6-311+G(3df,2p) Basis Set[a] of the Most Relevant Stationary Points on the Ground-State Potential Energy Surface for the 1,3-Migration in the Allylperoxyl Radical

structure[b]	UMP2	UCCSD(T)	RCCSD(T)
1A	0.0	0.0	0.0
TS1	38.8	27.4	23.2
		(28.0)[c]	(24.2)[c]
CX	20.7	20.2	
$C_3H_5^{\bullet} + O_2$	22.2	21.8	22.3
TS2	20.2	24.0	23.8
TS3	43.2	34.5	35.3
2A	−3.1	2.7	2.2

[a] Using the UMP2/6-311+G(3df,2p) optimized geometries. [b] See Figures 2−6. [c] Using the CASSCF(11,9)/6-311+G(3df,2p) optimized geometry.

Finally, the net atomic charges and atomic spin populations for these structures, calculated from AIM population analysis, are given in Table 4.

Allylperoxyl Radical Rotational Conformers. The allylperoxyl radical is a conformationally flexible system allowing torsion about the C1−C2 and C1−O4 bonds. Boyd et al.[10] have examined theoretically the conformational PES in **1a** employing single-point UMP2/6-31G(d,p) calculations, performed at the geometries optimized at the UHF/6-31G(d) level. Although it was not a central aim of the present study, we explored some conformational possibilities. We have found three conformational minima for **1a**, designated by **1A**, **1B**, and **1C** (Figure 2) which differentiates one from the others essentially in the value

Table 2. Relative Energies (kcal/mol) Calculated at Different Levels of Theory with the 6-311+G(3df,2p) Basis Set[a] of Selected Stationary Points on the Ground-State Potential Energy Surface for the 1,3-Migration in the Allylperoxyl Radical

structure[b]	CASSCF(11,9)	CASPT2
$C_3H_5^{\bullet} + O_2$	0.0	0.0
CX	0.7	−2.7
TS1	9.4	0.5
TS2	23.3	2.4

[a] Using the UMP2/6-311+G(3df,2p) optimized geometries, except **TS1** for which the CASSCF(11,3)/6-311+G(3df,2p) geometry was employed. [b] See Figures 3−5.

Table 3. Calculated Relative Energies (kcal/mol) of the Most Relevant Stationary Points on the Ground-State Potential Energy Surface for the 1,3-Migration in the Allylperoxyl Radical[a]

structure	ΔU^b	ΔE (0 K)	ΔH (298 K)	ΔG (298 K)
1A	0.0	0.0	0.0	0.0
TS1	24.2	21.5	21.7	21.0
CX	20.3	15.8	17.0	13.5
$C_3H_5^{\bullet} + O_2$	22.3	17.1	18.0	7.9
TS2	23.8	24.4	23.6	25.7
TS3	35.3	34.6	33.9	35.8
2A	2.2	1.2	2.6	2.3

[a] Using the UMP2/6-311+G(3df,2p) optimized geometries, except **TS1** for which the CASSCF(11,9)/6-311+G(3df,2p) geometry was employed. [b] Relative energy calculated at the RCCSD(T)/6-311+G(3df,2p) level. The relative energy of **CX** was obtained from the total energies of **CX** and $C_3H_5^{\bullet} + O_2$ calculated at the CASPT2/6-311+G(3df,2p) level, including the BSSE correction and the relative energy of $C_3H_5^{\bullet} + O_2$ with respect to **1A** calculated at the RCCSD(T)/6-311+G(3df,2p) level.

of the O5−O4−C1−C2 dihedral angle (i.e., 80.0°, −74.9°, and 171.3°, respectively). These structures are similar in geometry to those calculated by Boyd and co-workers, namely structures **F**, **D**, and **E**, respectively, in ref 10. At all levels of theory, structure **1A** is predicted to be the lowest energy conformation of **1a**, but the energies of the three minima differ in a few tenths of kcal/mol (Table S3, Supporting Information). Structure **1A** is therefore assigned an energy of zero, and energies of other structures through this paper are given relative to **1A**. According to Table 3, the enthalpy of reaction at 298 K, designated by ΔH_r(298 K), for the addition of triplet O_2 to the allyl radical to give **1A**, is predicted to be −18.0 kcal/mol. This value is in good agreement with the experimental ΔH_r(298 K) value of -18.2 ± 0.5 kcal/mol.[45] The **1A**, **1B**, and **1C** conformers of **1a** can be interconverted through rotation of the O4−O5 unit about the C1−O4 bond. We have found three transition structures, designated by **TSAB**, **TSAC**, and **TSBC** (Figure S1, Supporting Information), which differ again in the value of the O5−O4−C1−C2 dihedral angle (i.e., 3.5°, 131.1°, and −127.0°, respectively). The transition structures **TSAB**, **TSAC**, and **TSBC** correspond to structures **F** → **D**, **E** → **F**, and **D** → **E**, respectively, in ref 10. At all levels of theory (Table S3, Supporting Information), these transition structures lie within 2.5 kcal/mol of the equilibrium structure **1A**. As has previously been reported,[10] the three conformers **1A**−**1C** are polar, with dipole moments ranging from 2.78 D for **1B** to 3.07 D for **1C** (Table S2, Supporting Information). AIM population analysis indicates that in structure **1A** the peroxyl group carries an overall negative charge of 0.588 e and that the spin density is associated primarily with the terminal oxygen atom (O5) and the carbon atoms C2 and C3 (Table 4).

(45) Morgan, C. A.; Pilling M. J.; Tulloch, J. M. *J. Chem. Soc., Faraday Trans. 2* **1982**, *78*, 1323−1330.

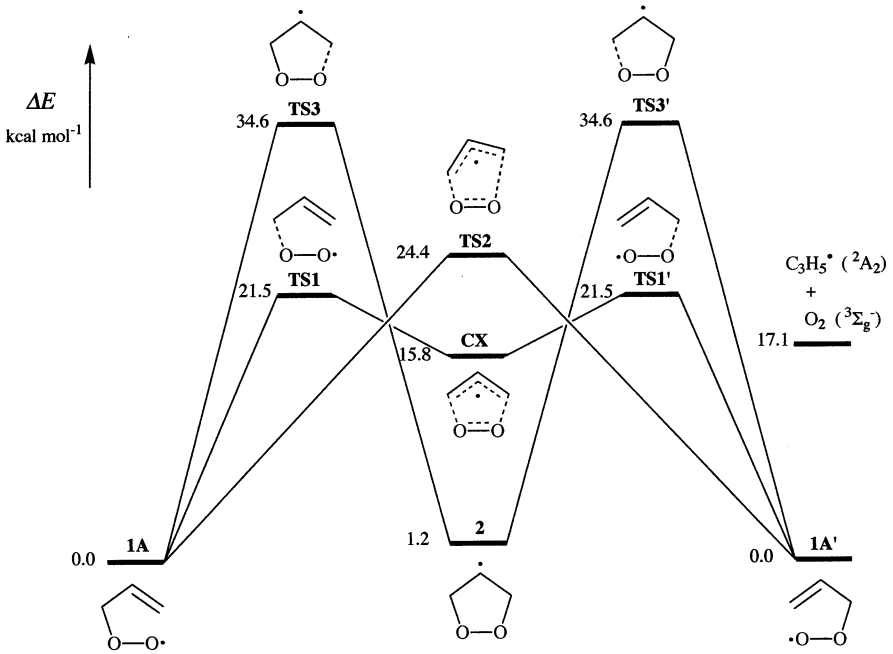

Figure 7. Schematic energy profiles along an arbitrary reaction coordinate showing the structures invoved in the three different pathways leading to the 1,3-migration in the allylperoxyl radical. Energy values obtained from ZPVE-corrected RCCSD(T)/6-311+G(3df,2p) total energies.

Table 4. Net Atomic Charges and Atomic Spin Populations Determined from AIM Population Analysis[a]

	net atomic charge					atomic spin population				
structure	C1	C2	C3	O4	O5	C1	C2	C3	O4	O5
1A	+0.447	-0.029	−0.037	-0.407	−0.181	+0.006	−0.535	+0.571	+0.330	+0.644
TS1	+0.061	+0.002	−0.052	−0.079	−0.149	−0.415	+0.000	−0.193	+0.856	+0.775
CX	−0.060	−0.009	−0.060	−0.013	−0.013	−0.519	+0.094	−0.519	+0.987	+0.987
TS2	+0.144	−0.018	+0.062	−0.161	−0.243	+0.144	−0.463	+0.498	+0.388	+0.451
TS3	+0.537	−0.024	+0.056	−0.563	−0.255	+0.014	+0.426	−0.080	+0.125	+0.502
2A	+0.516	−0.097	+0.519	−0.563	−0.564	+0.000	+0.858	+0.000	+0.007	+0.001

[a] Calculated by using the effective MP2/6-311+G(3df,2p) wave function. Atom numbering refers to Figures 2−6.

1,3-Migration in the Allylperoxyl Radical. Three reaction pathways for the 1,3-migration of the peroxyl unit in allylperoxyl radical have been found. The most favorable pathway (pathway **C** in Scheme 1) proceeds through the transition structure designated by **TS1** (Figure 3). Overall, the geometry of **TS1** optimized at the CASSCF level of theory is similar to that computed at the UMP2 level. Hence, in going from the UMP2 to the CASSCF geometry, the C1−O4 breaking bond is lengthened by 0.116 Å, whereas the C1−C2, C2−C3, and O4−O5 bonds are lengthened by less than 0.03 Å. Moreover, the RCCSD(T) energies calculated for **TS1** at the geometries optimized at the UMP2 and CASSCF levels of theory differentiate each other by 1.0 kcal/mol (Table 1). AIM population analysis reveals that the peroxyl moiety in **TS1** carries an overall negative charge of 0.228 e, which is substantially less than the corresponding value of 0.588 e in **1A** (Table 4).

The normal mode associated with the single imaginary vibrational frequency of **TS1** (966*i*) consisted mainly of an elongation of the C1−O4 distance combined with a rotation of the O4−O5 unit about the C1−O4 bond. A geometry reoptimization of **TS1**, slightly modified according to this normal mode with the appropriate sign, led to a structure which appears to be a loosely bound [C_3H_5 •···O_2] complex of C_s symmetry. The electronic ground-state state of this complex is a doublet of A″ symmetry, originating from the coupling of the $^2A_2$ state of the allyl radical with the $^3\Sigma_g^-$ state of O_2. The optimized geometry of the complex, **CX** (Figure 4), was characterized as a true minimum on the PES. The main geometrical features of **CX** are the long C−O distances (3.128 Å) and the insignificant structural changes of the allyl radical and dioxygen moieties in **CX** as compared with the separated species. Thus, in forming the **CX** complex, the C−C and O−O bonds undergo a lengthening of only 0.001 and 0.002 Å, respectively.

Figure 8 displays the electron charge density graph of **CX** in the plane containing the two oxygen atoms and the terminal carbon atoms of the allyl moiety. The presence of a bond critical point between atom pairs C1−O4 and C3−O5 indicates the existence of a binding interaction between these atom pairs. The relatively low value of the electron charge density ($\rho(r_b)$ = 0.0731 e bohr^{-3}) and the positive value of the its Laplacian ($\nabla^2\rho(r_b)$ = 0.023 e bohr^{-5}) and local electronic energy density ($E_e(r_b)$ = 0.0067 hartree bohr^{-3}) at these bond critical points (Table S4, Supporting Information) indicate that the atom pairs C1−O4 and C3−O5 are weakly bound by a closed shell interaction. It is remarkable the large value of the ellipticity of the C1−O4 and C3−O5 bonds (ϵ = 0.4528), which indicates an anisotropic distribution of the electron charge between these atom pairs. According to the net atomic charges calculated for the C1, C3, O4, and O5 atoms (Table 4), there is a small accumulation of negative charge within the basin of these atoms. Moreover, the net atomic charges on the oxygen atoms show an electron charge transfer of only 0.026 e in the direction

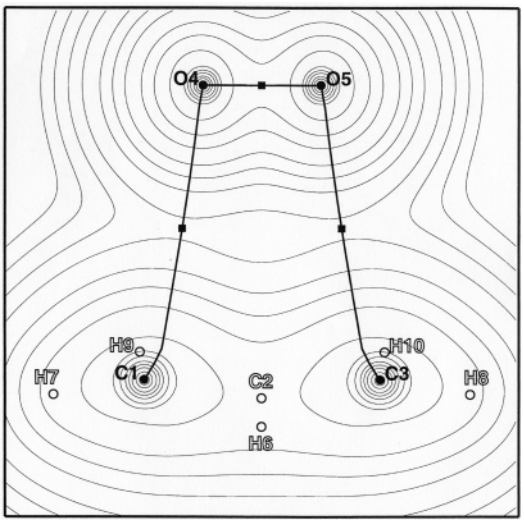

Figure 8. Contour plot in the C1−O4−O5−C3 plane and graph of the effective UMP2/6-311+G(3df,2p) electron charge density of the allyl radical−triplet dioxygen complex **CX**. Bond critical points are denoted by squares. The labels of the nuclei that lie in the C1−O4−O5−C3 plane are bold, and those that do not lie in this plane are open.

allyl → O_2. This is consistent with the abovementioned findings for the benzene−O_2 complex and again indicates that the dominant attractive interactions holding in association the allyl radical and O_2 partners in the loosely bound **CX** complex are due chiefly to dispersion forces.

At the UCCSD(T) level of theory, **CX** lies at 1.6 kcal/mol below the sum of the energies of the separated partners, $C_3H_5^\bullet$ + O_2 (Table 1). At this level of theory, a BSSE correction of 0.8 kcal/mol was calculated with the 6-311+G(3df,2p) basis set. This BBSE correction leads to a stabilization energy of only 0.8 kcal/mol of **CX** toward decomposition into $C_3H_5^\bullet$ + O_2. At this point, it is worth noting that the UHF wave function of the UMP2 and UCCSD(T) calculations with the 6-311+G(3df,2p) basis set was subjected to very serious spin contamination. Thus, the expected value of the S^2 operator was calculated to be 1.9811, as compared to 0.75 for a pure doublet state. This can be taken as an indication of strong nondynamical electron correlation effects. One may then question the reliability of the energy calculated for **CX** at the UCCSD(T) level of theory. On the other hand, the RCCSD(T) method cannot be employed for computing the energy of **CX** because the reference wave function cannot be described by a single ROHF determinant. In principle, a CASSCF approach should take into account the multiconfiguration character of the reference wave function and the nondynamical electron correlation effects in **CX**. However, since the dominant attractive interactions holding in association the allyl radical and O_2 partners in the **CX** complex arise mainly from dispersion forces, it is unlikely that the CASSCF method can provide an adequate description of this complex. In fact, the geometry reoptimization of structure **CX** at the CASSCF-(11,9) level of theory with the 6-311+G(3df,2p) basis set led to a five-membered ring structure showing two C−O bonds of 4.213 Å, which lies 0.1 kcal/mol below the energy of the isolated partners, $C_3H_5^\bullet$ + O_2. Therefore, an adequate description of the loosely bound **CX** complex requires a quantum mechanical method that can take into account both the dynamical and nondynamical electron correlation effects. Though the CASPT2 method fulfils these requirements, a geometry optimization at this level of theory with a large basis set is not currently possible for a system of the size of structure **CX** because analytical CASPT2 energy gradients are not available in the MOLCAS program package. Therefore, we decided to evaluate the CASPT2 energy of **CX** employing the geometry optimized at the UMP2 level. According to Table 2, at the CASPT2 level of theory, **CX** lies at 2.7 kcal/mol below the sum of the energies of the separated partners, $C_3H_5^\bullet$ + O_2. At this level of theory, a BSSE correction of 0.7 kcal/mol was calculated. This BBSE correction reduces the predicted stabilization energy to 2.0 kcal/mol. Inclusion in the latter value of a ZPVE correction of 0.7 kcal/mol leads to a 0 K stabilization energy of 1.3 kcal/mol of **CX** toward decomposition into $C_3H_5^\bullet$ + O_2. This predicted stabilization energy should be considered as a lower value because the geometry of the complex was optimized at the UMP2 rather than at the CASPT2 level of theory.

Our best relative energy of **CX** with respect to the energy of **1A** (i.e., 20.3 kcal/mol, Table 3) was obtained from the total energies of **CX** and $C_3H_5^\bullet$ + O_2 calculated at the CASPT2/6-311+G(3df,2p) level, including the BSSE correction, and the relative energy of $C_3H_5^\bullet$ + O_2 with respect to the energy of **1A** calculated at the RCCSD(T)/6-311+G(3df,2p) level. According to Table 3, the ΔH_r(298 K) for the process **1A** → **CX** is predicted to be 17.0 kcal/mol. This elementary reaction involves an enthalpy of activation at 298 K, designated by $\Delta H^{\ddagger}$(298 K), of 21.7 kcal/mol. Since the transition structure for the formation of **CX** from **1A** (**TS1**) and the transition structure for the formation of the rearranged peroxyl radical **1A′** (**TS1′**) are degenerate, it is concluded that the overall $\Delta H^{\ddagger}$(298 K) for the **1A** → **1A′** rearrangement via pathway **C** (Scheme 1) is predicted to be 21.7 kcal/mol.

We have found a transition structure for the concerted rearrangement of **1a** to **1a′** (pathway **B** in Scheme 1). This five-membered ring transition structure, designated by **TS2** (Figure 5), shows an elongated breaking C−O bond of 1.777 Å and a long forming C−O bond of 2.048 Å. The normal mode associated with the single imaginary vibrational frequency of **TS2** (519*i*) corresponds chiefly to a shortening of one of these C−O bonds and a lengthening of the other one, i.e it leads to either the **1B** conformational minimum of **1a** or to its rearranged structure (**1B′**). We should point out that Boyd and co-workers[10] did not find any transition structure for the concerted rearrangement (pathway **B** in Scheme 1) at the UHF/6-31G(d) level. Our results suggest that a proper description of the transition structure for the concerted pathway **B** requires the explicit incorporation of the electron correlation effects in the computational method employed. Thus, we were not able to compute **TS2** by using a UHF wave function with neither the 6-31G(d) nor 6-311+G-(3df,2p) basis sets. On the other hand, by using the spin-unrestricted version of the configuration interaction with all single and double excitations (CISD)[46] and quadratic CISD (QCISD)[47] methods, we did locate a transition structure for the concerted pathway **B** showing a geometry close to that computed with the UMP2 method. In clear contrast, several attempts to locate such a transition structure with the spin-unrestricted version of the DFT Becke three-parameter hybrid functional[48]

(46) Pople, J. A.; Seeger, R.; Krishnan, R. *Int. J. Quantum. Chem. Symp.* **1977**, *11*, 149.
(47) Pople, J. A.; Head-Gordon, M.; Raghavachari, K. *J. Chem. Phys.* **1987**, *87*, 5968.
(48) Becke, A. D. *J. Chem. Phys.* **1993**, *98*, 5648.

combined with the Lee, Yang, and Parr (LYP) correlation functional,[49] designated by UB3LYP,[50] were unsuccessful. Similar failures of the UB3LYP functional were also observed in recent theoretical studies on the mechanism of the oxidation of alkyl radicals by O_2.[51,52]

The UMP2 and UCCSD(T) calculations show that the energy of **TS2** lies below that of **TS1** (Table 1). However, the RCCSD(T) calculations reverse the relative energy ordering and **TS2** is found to be 0.6 kcal/mol *more* energetic than **TS1**. Inclusion of the ZPVE corrections increases this small energy difference to 2.9 kcal/mol. According to Table 3, the concerted 1,3-migration in **1A** through **TS2** involves an $\Delta H^{\ddagger}$(298 K) of 23.6 kcal/mol, whereas the two-step 1,3-migration via **TS1** involves an $\Delta H^{\ddagger}$(298 K) of 21.7 kcal/mol. Therefore, on the basis of the calculated $\Delta H^{\ddagger}$(298 K) it can be concluded that pathway **C** is more favorable than pathway **B** (Scheme 1) by 1.9 kcal/mol. Furthermore, this conclusion is confirmed by the Gibbs free energies of activation at 298 K, designated by $\Delta G^{\ddagger}$(298 K), of 21.0 and 25.7 kcal/mol calculated for pathways **C** and **B**, respectively (Table 3).

Finally, we find that the ring closure of **1a** to give **2a** (pathway **A** in Scheme 1) proceeds through the transition structure designated by **TS3** (Figure 6). This five-membered ring transition structure shows a short C−O bond of 1.426 Å and a long forming C−O bond of 1.976 Å. Overall, the geometry of **TS3** is similar to that computed by Boyd and co-workers at the UHF/6-31G(d) level (structure **N** in ref 10). A comparison of AIM population analysis for the cyclic transition structures **TS3** and **TS2** reveals that the peroxyl moiety in **TS3** carries an overall negative charge of 0.818 e, while in that in **TS2** carries a negative charge of only 0.404 e. Thus, **TS3** is predicted to be more polar than **TS2**. This prediction is consistent with the calculated electric dipole moments of 1.57 and 2.90 D for **TS2** and **TS3**, respectively (Table S2, Supporting Information).

The atomic displacements associated to the one imaginary vibrational frequency of **TS3** (964*i*) is dominated by a lengthening (or shortening) of the C3−O5 distance. A geometry reoptimization of **TS3**, slightly modified according to this normal mode with the appropriate sign, led to a puckered nonsymmetric (C_1) five-membered ring structure, designated by **2A** (Figure 6), which turns out to be the lowest energy conformation of dioxolanyl radical **2a**. We explored other conformational possibilities for **2a**. Besides structure **2A**, we have found a structure with C_2 symmetry, designated by **2B**, and another structure with C_s symmetry, designated by **2C** (Figure S2, Supporting Information). At the RCCSD(T) level of theory, the energy of **2B** is calculated to be only 0.001 kcal/mol higher than that of **2A**, whereas the energy of **2C** is calculated to be higher than that of **2A** by 4.5 kcal/mol (Tables S2 and S3, Supporting Information). However, structures **2B** and **2C** are not true energy minima on the conformational PES because a vibrational analysis revealed that both structures have one imaginary frequency. AIM population analysis indicates that in structure **2A** the majority of the spin density resides at the central carbon atom (C2) and that the peroxyl group carries an overall negative charge of 1.127 e (Table 4). Thus, in passing from the peroxyl **1A** to the dioxolanyl radical intermediate **2A**, the overall negative charge carried by the peroxyl moiety increases by 0.539 e. However, the electric dipole moment increases by only 0.08 D (Table S2, Supporting Information). Therefore, both free radicals show a similar polar character.

Table 5. Solvent Effect on the Energies (kcal/mol) of Selected Stationary Points on the Ground-State Potential Energy Surface for the 1,3-Migration in the Allylperoxyl Radical[a]

structure	heptane	water
1A	−1.5	−3.0
TS1	−0.9	−0.8
CX	0.7	2.8
$C_3H_5^{\bullet} + O_2$	0.0	2.5
TS2	−2.1	−3.9
TS3	−2.7	−6.8
2A	−3.8	−10.8

[a] Calculated with the PCM method at the UMP2 level of theory with the 6-311+G(3df,2p) basis set using the geometries optimized in gas phase at the UMP2/6-311+G(3df,2p) level.

The UMP2 calculations predict the ring closure **1A** → **2A** to be exoergic by 3.1 kcal/mol (Table 1). However, the RCCSD(T) calculations indicate that this reaction is slightly endoergic. Further, the ΔH_r(298 K) for the ring closure **1A** → **2A** is predicted to be 2.6 kcal/mol (Table 3). At the UMP2/6-311+G(3df,2p) level, **TS3** lies 43.2 kcal/mol above **1A** (Table 1). This potential energy barrier is 2.9 kcal/mol higher than that obtained by Boyd and co-workers from UMP2/6-31G(d,p) calculations employing UHF/6-31G(d) optimized geometries.[10] According to Table 3, the formation of **2A** via **TS3** involves a $\Delta H^{\ddagger}$(298 K) of 33.9 kcal/mol. Therefore, the sequence of ring closure **1a** → **2a** and ring opening **2a** → **1a′** (pathway **A** in Scheme 1) is unlikely to play any significant role in the allylperoxyl rearrangement **1a** → **1a′**. This result is in agreement with most experimental studies[5−7] and Boyd's previous theoretical study.

Solvent Effects on the 1,3-Migration in the Allylperoxyl Radical. To investigate the possible solvent-induced changes on the preferred pathway for the 1,3-migration in the allylperoxyl radical, the solvent effects were introduced within the self-consistent reaction field (SCRF) formalism by means of the polarized continuum model (PCM) of Tomasi et al.[53] as implemented in GAUSSIAN 98. All SCRF calculations were carried out at the UMP2 level of theory with the 6-311+G(3df,2p) basis set using optimized gas-phase molecular geometries computed at the same level of theory. Despite the fact that the allylperoxyl radical rearrangements are experimentally performed in nonpolar aprotic solvents, two different continuum environments characterized by relative dielectric permittivities of 1.92 (heptane) and 78.39 (water) were considered to explore the influence of increasing the dielectric permittivity on the potential energy barrier of the different reaction pathways studied.

The solvent effect on the energies of the most relevant stationary points of the ground-state PES for the 1,3-migration in **1a**, evaluated as the difference between the total energies calculated in the solvent and in the gas phase, are summarized in Table 5. In the three pathways investigated, it is found that the energies of the corresponding transition structures are lower

(49) Lee, C.; Yang, W.; Parr, R. G. *Phys. Rev. B* **1988**, *37*, 785.
(50) Stevens, P. J.; Devlin, F. J.; Chablowski, C. F.; Frisch, M. J. *J. Phys. Chem.* **1994**, *98*, 11623.
(51) Bofill, J. M.; Olivella, S.; Sole, A.; Anglada, J. M. *J. Am. Chem. Soc.* **1999**, *121*, 1337−1347.
(52) Olivella, S.; Bofill, J. M.; Sole, A. *Chem.−Eur. J.* **2001**, *7*, 3377−3386.
(53) (a) Miertus, S.; Scrocco, E.; Tomasi, J. *Chem. Phys.* **1981**, *55*, 117. (b) Miertus, S.; Tomasi, J. *Chem. Phys.* **1982**, *65*, 239. (c) Tomasi, J.; Persico, M. *Chem. Rev.* **1994**, *94*, 2027.

in heptane solution than in the gas phase. This energy lowering is, however, rather small for **TS1**. Thus, while **TS3** and **TS2** undergo an energy stabilization of 2.7 and 2.1 kcal/mol, respectively, the energy of **TS1** is lowered by only 0.9 kcal/mol. Nevertheless, since the difference between the $\Delta G^{\ddagger}$(298 K) calculated for the pathways through the transition structures **TS1** and **TS2** (i.e., pathways **C** and **B** in Scheme 1) is 4.7 kcal/mol (Table 3), it is unlikely that in nonpolar aprotic solvents the larger stabilization of 1.2 kcal/mol evaluated for **TS2**, as compared to **TS1**, may reverse the predicted preference of pathway **C** over pathway **B** in the gas phase.

In aqueous solution, an energy lowering is found also for the three transition structures **TS1**, **TS2**, and **TS3**. Again the largest energy lowerings are found for **TS3** (6.8 kcal/mol) and **TS2** (3.9 kcal/mol), whereas the stabilization for **TS1** (0.8 kcal/mol) appears to be very small. When the high polarity of water is taken into account, these findings can be rationalized in terms of the increase in the charge separation between the peroxyl and allyl moieties in the transition structures **TS1**, **TS2**, and **TS3**. Thus, according to the net atomic charges displayed in Table 4, the overall negative charge carried by the peroxyl moiety increases in the order **TS1** (0.228 e) < **TS2** (0.404 e) < **TS3** (0.818 e). In this regard, it is worth noting that the energy of complex **CX** in both the gas phase and heptane solution is predicted to be lower than in water. This result is consistent with the small negative charge of 0.026 e residing in the dioxygen unit of **CX** (Table 4). Again, it is not expected that the larger stabilization of 3.1 kcal/mol found for **TS2**, as compared to **TS1**, in aqueous solution may compensate for the larger difference in $\Delta G^{\ddagger}$(298 K) of 4.7 kcal/mol calculated for the first transition structure. In conclusion, it is very unlikely that the solvent effects may reverse the predicted preference of pathway **C** over pathway **B** in the allylperoxyl rearrangement.

Summary and Conclusions

In this paper, we have investigated by means of quantum mechanical electronic structure calculations the three pathways most often suggested for 1,3-migration of the peroxyl group in the allylperoxyl radical, **1a**, a key reaction involved in the spontaneous autoxidation of unsaturated lipids of biological importance. The following points emerge from this investigation:

(1) According to the barrier heights calculated from RCCSD(T)/6-311+G(3df,2p) energies with optimized molecular geometries and harmonic vibrational frequencies determined at the UMP2/6-311+G(3df,2p) level, the allylperoxyl rearrangement proceeds by fragmentation of **1a** through a transition structure, **TS1**, to give an allyl radical−triplet dioxygen loosely bound complex, **CX**. In a subsequent step, the triplet dioxygen moiety of **CX** recombines at either end of the allyl radical moiety to convert the complex to the rearranged peroxyl radical (**1a′**) or to revert to the starting peroxyl radical **1a** (pathway **C** in Scheme 1). The overall $\Delta H^{\ddagger}$(298 K) of this pathway is calculated to be 21.7 kcal/mol.

(2) The loosely bound complex **CX** shows two long C−O distances of 3.128 Å and an electron charge transfer of only 0.026 e in the direction allyl → O_2. The ΔH(298 K) for dissociation of **CX** in its isolated partners, allyl radical and triplet dioxygen, is predicted to be at least 1 kcal/mol. The dominant attractive interactions holding in association the allyl radical−triplet dioxygen pair in **CX** are due chiefly to dispersion forces.

(3) The observed high degree of stereoselectivity of the rearrangement results from the formation of the **CX** complex, which prevents the diffusion of the allyl radical and triplet dioxygen partners and maintains the stereocontrol along the fragmentation−recombination processes.[54]

(4) The concerted 1,3-migration in the allylperoxyl radical (pathway **B** in Scheme 1) is predicted to take place through a five-membered ring transition structure, **TS2**, showing two long C−O bonds. Though the potential energy calculated for **TS2** is 0.4 kcal/mol lower than that calculated for **TS1**, the $\Delta H^{\ddagger}$(298 K) determined for pathways **B** and **C** indicates that the fragmentation−recombination pathway **C** is more favorable than the concerted pathway **B** by 1.9 kcal/mol.

(5) The cyclization of the allylperoxyl radical to produce a dioxolanyl radical intermediate, **2a**, is found to proceed through a five-membered ring transition structure, **TS3**, showing a long C−O bond. Since the $\Delta H^{\ddagger}$(298 K) for this cyclization is calculated to be 33.9 kcal/mol, it is concluded that the sequence of ring closure **1a** → **2a** and ring opening **2a** → **1a′** (pathway **A** in Scheme 1) is unlikely to play any significant role in the allylperoxyl rearrangement **1a** → **1a′**.

(6) In the three pathways investigated, the energies of the corresponding transition structures are predicted to be somewhat lower in both heptane and aqueous solution than in the gas phase. Despite that the energy lowering calculated for **TS1** is smaller than the calculated for **TS2** and **TS3**, it is very unlikely that the solvent effects may reverse the predicted preference of pathway **C** over pathways **B** and **A** in the gas phase.

Acknowledgment. This research was supported by the Spanish DGICYT (Grants PB98-1240-C02-01, BQU2002-04485-C02-01, and BQU2002-04485-C02-02). Additional support came from Catalonian CIRIT (Grant 2001SGR00048). Calculations described in this work were performed on a HP9000 J282 workstation at the University of Barcelona and on the CPQ AlphaServer HPC320 at the Centre de Supercomputació de Catalunya (CESCA).

Supporting Information Available: Cartesian coordinates of all structures reported in this paper, Tables S1−S4 summarizing total energies, zero-point vibrational energies, electric dipole moments, topological properties of bond critical points, and Figures S1 and S2 of additional stationary points. This material is available free of charge via the Internet at http://pubs.acs.org.

JA030171E

(54) In relation to the interpretation of the experiments that describe the stereochemical transfer of chiriality in the allylperoxyl rearrangement, an anonymous referee has raised the question of whether calculations on the difference in energy of the complex **CX** having a methyl substituent on C1 in the two possible orientations (i.e., pseudo trans and pseudo cis to the C2−C3 bond) would explain the overall stereochemical outcome. To investigate this interesting point, we have carried out preliminary calculations on the relative energies of the pseudo trans and pseudo cis methyl substituted complex **CX**. At the UMP2 level of theory with the 6-311+G(2df,p) basis set, including the ZPVE correction, the pseudo trans conformation turns out to be 0.5 kcal/mol less energetic than the pseudo cis one. This results account for two important experimental facts (ref 12b): (1) while the allylperoxyl rearrangement is highly stereoselective, the rearrangements starting from an allylperoxyl radical having a cis substituent in the double bond occur with les stereoselectivity than rearrangements proceeding from an allylperoxyl radical having a trans substituent, and (2) rearrangements across a trans double bond occur more readily than rearrangements across a cis double bond. Following another interesting suggestion by the same anonymous referee, we have carried out additional calculations on the relative energies of the complex **CX** having a methyl substituent on both C1 and C3 in the three possible orientations (i.e., trans−trans, trans−cis, and cis−cis). At the UMP2/6-311+G(2df,p) plus ZPVE correction, the relative energies of these structures are found to be 0.0, 0.5, and 3.7 kcal/mol, respectively. Therefore, these results nicely agree with the aforementioned experimental findings.